

# Double Privacy Guard: Robust Traceable Adversarial Watermarking against Face Recognition

Yunming Zhang, Dengpan Ye, Sipeng Shen, Caiyun Xie, Ziyi Liu, Jiacheng Deng, Long Tang

**Abstract**—The wide deployment of Face Recognition (FR) systems poses risks of privacy leakage. One countermeasure to address this issue is adversarial attacks, which deceive malicious FR searches but simultaneously interfere the normal identity verification of trusted authorizers. In this paper, we propose the first Double Privacy Guard (DPG) scheme based on traceable adversarial watermarking. DPG employs a one-time watermark embedding to deceive unauthorized FR models and allows authorizers to perform identity verification by extracting the watermark. Specifically, we propose an information-guided adversarial attack against FR models. The encoder embeds an identity-specific watermark into the deep feature space of the carrier, guiding recognizable features of the image to deviate from the source identity. We further adopt a collaborative meta-optimization strategy compatible with sub-tasks, which regularizes the joint optimization direction of the encoder and decoder. This strategy enhances the representation of universal carrier features, mitigating multi-objective optimization conflicts in watermarking. Experiments confirm that DPG achieves significant attack success rates and traceability accuracy on state-of-the-art FR models, exhibiting remarkable robustness that outperforms the existing privacy protection methods using adversarial attacks and deep watermarking, or simple combinations of the two. Our work potentially opens up new insights into proactive protection for FR privacy.

## I. INTRODUCTION

Face Recognition (FR) systems are widely used in criminal investigations, security surveillance, and online monitoring, providing significant convenience to social networks. The effectiveness of FR systems also poses a threat to privacy protection [1]. When Personal Users (PUs) upload the facial image to social networks, Trusted Authorizers (TAs) (e.g., network administrators and law enforcement agencies) can use the FR system to authenticate facial image. However, Unauthorized Adversaries (UAs) may also use open source FR systems for malicious FR search of PUs' face images, leading to user privacy leakage. Therefore, there is an urgent need to develop a comprehensive facial image privacy protection method that safeguards PUs' facial images from malicious recognition search by UAs without affecting legitimate authentication processes, as illustrated in Figure 1.

One countermeasure to address privacy security concerns is adversarial attacks, which deceive FR models by introducing visible patches [2], [3] or invisible perturbations [4], [5] in images. However, these methods exhibit certain drawbacks, including poor black-box transferability, lack of robustness, and significant semantic modifications to protected images [6], thereby affecting their practical applications in social network scenarios. Most importantly, adversarial attacks irreversibly disrupt the recognizable features of facial images. While this

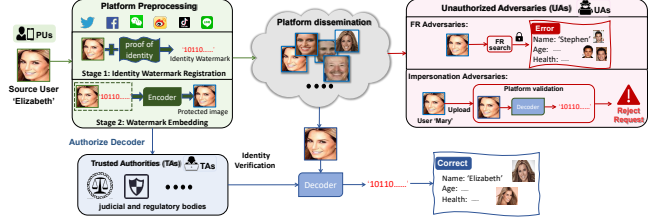


Fig. 1. Illustration of DPG protection scenario. Users can upload the encoded and protected facial image to social networks, deceiving unauthorized malicious face recognition. Meanwhile, TAs can perform identity authentication on the image for security investigation.

prevents malicious recognition by UAs, it also hinders normal identity verification by TAs, potentially leading to security and regulatory vulnerabilities.

Adversarial attacks in the privacy protection scenario have prompted an innovative question: Can we transform adversarial examples into verifiable patterns for TAs' identity verification while deceiving unauthorized FR models? Deep watermarking methods offer a new perspective for verifiable adversarial examples [7], which typically protect the copyright of digital media by invisibly embedding traceable watermarks. The watermark encoder learns the embedding of watermarks in the deep feature space of images to enhance robustness, enabling deployment in complex social network scenarios. However, traditional deep watermark algorithms fail to disrupt malicious face recognition, thus unable to fundamentally address privacy leakage issues.

In this paper, we propose the first Double Privacy Guard (DPG) scheme based on robust and traceable adversarial watermarking. By one-time embedding identity-specific watermarks into source images, DPG deceives unauthorized face recognition while permitting TAs to extract watermarks for identity verification. A comparison of DPG with existing works is shown in Table I. DPG focuses on the following three challenges to achieve comprehensive privacy protection: **1) Traceable and adversarial dual-effectiveness**: We introduce an information-guided adversarial attack strategy against FR models. This strategy embeds an identity-specific watermark into the source image using the encoder, guiding the recognizable features of the source image to map onto the target feature domain, deceiving FR models. **2) Transferability to black-box FR models**: There is an optimization conflict between the adversariality and invisibility of watermarks. Adversariality enhancements under single-model or basic ensemble overly penalize image quality and lack transferability to black-box FR models. Therefore, we adopt a meta-learning strategy in

the multi-task end-to-end optimization, calibrating training errors across distinct tasks, thereby enhancing the encoding of universal carrier features. **3) Model robustness against common image processing:** We add a simulated noise pool and design regularization under temporary encoder parameters to adjust the optimization direction of the decoder. This enhances the robustness of the decoder and facilitates the synergistic optimization between the encoder and decoder. Furthermore, multi-task training contributes to the overall robustness of the model.

Our contributions are summarized as follows:

- We propose DPG, the first dual-effect privacy protection scheme based on traceable adversarial watermarking, which simultaneously attacks unauthorized FR models while allowing image identity verification by TAs.
- We innovatively present an information-guided adversarial attack method against FR models, which maps recognizable features of the image to the target domain through identity-specific watermarks, influencing the facial feature reconstruction of FR models.
- We adopt the collaborative meta-optimization strategy compatible with diverse tasks to enhance the universal feature encoding of the carrier, mitigating optimization conflicts between adversariality and invisibility.
- We conduct extensive experiments on two large facial datasets against six SOTA offline FR models and two online commercial FR systems, validating the significant transferability, traceability and robustness of DPG.

## II. RELATED WORKS

### A. Adversarial Attacks against Face Recognition

Studies have demonstrated the vulnerability of FR models to adversarial examples. White-box attacks [8] and query-based black-box attacks [3] heavily depend on model accessibility, rendering them impractical for real-world applications. Therefore, more privacy protection methods are focusing on black-box attacks. [9] propose AdvHat, a real-world adversarial attack using sticker on the hat. [10] enhance the black-box transferability of adversarial attacks through synthesizing eye makeup patches. To eliminate vulnerabilities arising from low-level pixel modifications and enhance transferability to black-box FR models, some studies design perturbation-based attack methods with PGD [11] or FGSM [12] as underlying optimization algorithms. [13] increase the diversity of surrogate models and obtain ensemble-like effects, significantly improving the transferability. [4] enhances transferability by selecting a attribute recognition task related to FR. However, the perturbation-based methods directly overlay gradients in the pixel domain of the carrier, lacking robustness. In essence, adversarial attacks irreversibly disrupt recognizable features essential for FR, thereby hindering normal identity verification by authorizers and impacting the compliant security oversight.

### B. Deep Watermarking

Deep watermarking is extensively employed for copyright tracking in digital media. Recent studies have proposed utilizing deep watermarking methods to enhance the security of

Method	Type	Adversariality			Traceability	
		Original	Transferability	Robust	Original	Robust
Adv-Makeup [10]	Patch	✓	✓	✗	✗	✗
AdvHat [9]	Patch	✓	✗	✗	✗	✗
PGD [11]	Perturbation	✓	✓	✗	✗	✗
FGSM [12]	Perturbation	✓	✓	✗	✗	✗
Hidden [7]	Watermark	✗	✗	✗	✓	✓
FakeTagger [14]	Watermark	✗	✗	✗	✓	✓
<b>DPG (ours)</b>	Watermark	✓	✓	✓	✓	✓

TABLE I

COMPARISONS OF RELEVANT RESEARCH ON PRIVACY PROTECTION.

facial images. [14] utilize the deep watermarking method to encode watermarks into carrier face images, enabling effective tracing of deeply manipulated facial images. [15] introduce Artificial Fingerprints, which tracks facial images by transferring fingerprints from training data to the deep forgery model. Visible watermarks are employed for annotating copyright information and attacking classification models [16], [17]. However, they are not suitable for privacy protection in facial image scenarios. The watermark encoder deeply embeds watermark information into the robust features of the carrier, and through end-to-end training, it learns the globally optimal solution of the encoder and decoder. This inspires us to design a dual-effect privacy protection scheme for complex social network scenarios on this basis. By defining an information-guided adversarial attack, it can avoid the irrecoverable issue of adversarial perturbations, enabling TAs to decode the watermark for identity verification.

## III. THREAT MODEL

We define a threat model in terms of the potential processing of facial images in propagation, considering three entities with different knowledge and capabilities:

**PU:** Possessing a personal image set  $x_s \in \mathbb{R}^{i \times h \times w}$  and a unique watermark  $w_{id} \in [0, 1]^{1 \times l}$  representing personal identity, where  $\mathbb{R}$  is a real field of dimension  $i \times h \times w$  and  $l$  represents the length of the watermark. PUs defaults to unified management by TAs and have no knowledge of the structure and parameters of FR models possessed by UAs.

**UAs:** They can acquire facial images of PUs on social networks, verifying the identity of the images through open-source FR systems  $\mathcal{F}(\cdot)$  to obtain relevant privacy data.

**TAs:** Represented by security supervision personnel or network administrators, TAs verify the identity of facial images when conducting investigations and collecting evidence.

Users can utilize DPG to protect image privacy. Initially, PUs train the encoder  $\mathcal{E}(\cdot)$  and decoder  $\mathcal{D}(\cdot)$  of DPG by selecting a target person image  $x_t \in \mathbb{R}^{1 \times h \times w}$  with the different identity for impersonation attack. Before uploading images to social networks, PUs can embed watermarks into images using the trained encoder and authorize the decoder for TAs:

$$\hat{x}_s = \mathcal{E}(x_s, w_{id}). \quad (1)$$

The watermark does not impact the social usability of the carrier, PUs can share the watermarked image  $\hat{x}_s$  on networks. When UAs perform malicious facial comparisons on  $\hat{x}_s$ , the adversariality of  $\hat{x}_s$  causes the FR model to confidently

---

**Algorithm 1** DPG Training Framework
 

---

**Require:**  $x_s$  (training original source image);  $w_{id}$  (watermark ID);  $\mathcal{E}(\cdot)$  (watermark encoder);  $\mathcal{D}(\cdot)$  (watermark decoder);  $\mathcal{F}_p \in \{\mathcal{F}_1, \mathcal{F}_2 \dots \mathcal{F}_P\}$  (FR models for meta training);  $\mathcal{F}_q \in \{\mathcal{F}_1, \mathcal{F}_2 \dots \mathcal{F}_Q\}$  (FR models for meta testing);

**Ensure:** best model parameters;

- 1: Initialization;
- 2: **for**  $i \in [0, maxiter]$  **do**
- 3:    $\hat{x}_s \leftarrow \mathcal{E}(x_s, w_{id})$ ;
- 4:   **for**  $p \in P$  **do**
- 5:      $\hat{E}_s, E_t \leftarrow \mathcal{F}_p(\hat{x}_s, x_t)$ ;
- 6:     Calculate  $\mathcal{L}_{inv}^{\phi_{en}}$  and  $\mathcal{L}_{adv}^{tra}$  with Eq.5&8;
- 7:      $\theta^p \leftarrow \phi_{en} - \eta \nabla_{\phi_{en}} \mathcal{L}_{adv}^{tra}$ .
- 8:     **for**  $q \in Q$  **do**
- 9:       $\hat{x}_{s\_tes} \leftarrow \mathcal{E}(x_s, w_{id} | \theta^p)$ ;
- 10:      Calculate  $\mathcal{L}_{adv}^{tes}$  and  $\mathcal{L}_{inv}^{tes}$  with Eq.11&12;
- 11:     **end for**
- 12:   **end for**
- 13:   Calculate  $\mathcal{L}_{inv}^{total}$  and  $\mathcal{L}_{adv}^{total}$  with Eq.13&14;
- 14:   Calculate  $\mathcal{L}_{wm}^{total}$  and  $\mathcal{L}_{total}$  with Eq.17& 18;
- 15:   Update  $\mathcal{E}(\phi_{en})$  and  $\mathcal{D}(\cdot)$ ;
- 16: **end for**
- 17: **return** best model parameters;

---

identify  $\hat{x}_s$  and  $x_t$  as the same identity, thereby protecting the true identity information. Simultaneously, TAs can extract the watermark for identity verification without impacting normal security investigation and evidence collection:

$$\hat{w}_{id} = \mathcal{D}(\hat{x}_s). \quad (2)$$

Given the threat scenario, the practical application of DPG necessitates optimization training in three aspects: (1) *Invisibility optimization*: ensuring the watermark does not significantly affect the visual quality of the carrier; (2) *Adversarial optimization*: enabling the watermarked image to disrupt unknown FR models; (3) *Traceability optimization*: ensuring the decoder accurately extracts the watermark. These three optimization objectives can be formalized as follows:

$$\begin{cases} \min_{\mathcal{E}}(\mathcal{L}(\mathcal{E}(x_s), x_s)), & \text{invisibility optimization,} \\ \min_{\mathcal{E}}(\mathcal{L}(\mathcal{F}(\hat{x}_s), \mathcal{F}(x_t))), & \text{adversarial optimization,} \\ \min_{\mathcal{D}}(\mathcal{L}(\mathcal{D}(\hat{x}_s), w_{id})), & \text{traceability optimization,} \end{cases} \quad (3)$$

where  $\mathcal{L}$  represents the corresponding loss functions, which will be elaborated in the next section.

#### IV. METHODOLOGY

In this section, we provide a detailed explanation of the proposed pipeline and the architecture is depicted in Figure 2.

##### A. Information-Guided Adversarial Attack

The DPG encoder is designed to embed identity-specific watermark into the source image, mapping the recognizable features of the source image to the target identity feature

domain, to disrupt the decision of FR models. The backbone network of the encoder is designed based on MBRS [18]. We first encode the deep adversarial features of the carrier through the encoder. To seamlessly embed the watermark into the encoded carrier feature map and enhance the fault tolerance of the watermark, we introduce redundancy to the watermark through a two-dimensional convolutional layer with a stride of 2, expanding it to the same dimension as the carrier. As watermark information is connected to the feature map in the channel dimension, we introduce the CBAM module [19] to enhance the CNN-based encoding architecture. By explicitly modeling interdependencies between channels and spatial dimensions, CBAM module adaptively recalibrates feature responses to determine the optimal watermark embedding strength.

The watermark encoder  $\mathcal{E}(\cdot)$  receives the original face image  $x_s$  along with the watermark  $w_{id}$  representing its identity and encodes them under initialized parameters  $\phi_{en}$ :

$$\hat{x}_s = \mathcal{E}(x_s, w_{id} | \phi_{en}). \quad (4)$$

To enhance the generalization capability of the DPG encoder and decoder and avoid overfitting, we generate a random watermark for each batch during training. Users can customize  $w_{id}$  for one or more images during the inference process. To limit the impact of watermark encoding on the carrier, we use MSE loss  $\mathcal{L}_{MSE}$  to define the image invisibility loss  $\mathcal{L}_{inv}^{\phi_{en}}$ :

$$\mathcal{L}_{inv}^{\phi_{en}} = \mathcal{L}_{MSE}(x_s, \hat{x}_s). \quad (5)$$

To make the traceable watermark adversarial against FR models, we introduce adversarial constraints to optimize the encoder. FR model attacks can be categorized into two types: untargeted (dodging) and targeted (impersonation) attacks. Unlike dodging attack lowering similarity confidence for same-identity pairs, impersonation attack aims to enhance feature similarity between target and source images of different identities [10]. This method seamlessly incorporate the watermark model into end-to-end optimization and disrupt the feature reconstruction of FR models. Therefore, we focus on impersonation attacks as in [1], [4], [10].

To achieve the mapping of recognizable features from the watermarked image to the target domain, we first obtain recognizable feature embeddings  $E_*$  from the FR model for both the watermarked image and the target image, as follows:

$$\hat{E}_s, E_t = \mathcal{F}(\hat{x}_s, x_t). \quad (6)$$

These features are then used to calculate the adversarial loss  $\mathcal{L}_{adv}$  for targeted attacks. We employ cosine similarity loss [20] to calculate  $\mathcal{L}_{adv}$ :

$$\mathcal{L}_{adv} = 1 - \cos(\hat{E}_s, E_t). \quad (7)$$

Existing research has demonstrated that multitask learning improves adversarial robustness while maintaining single-task performance [21]. This further motivates the expansion of the output dimensions of the watermarking model by incorporating adversarial attack tasks.

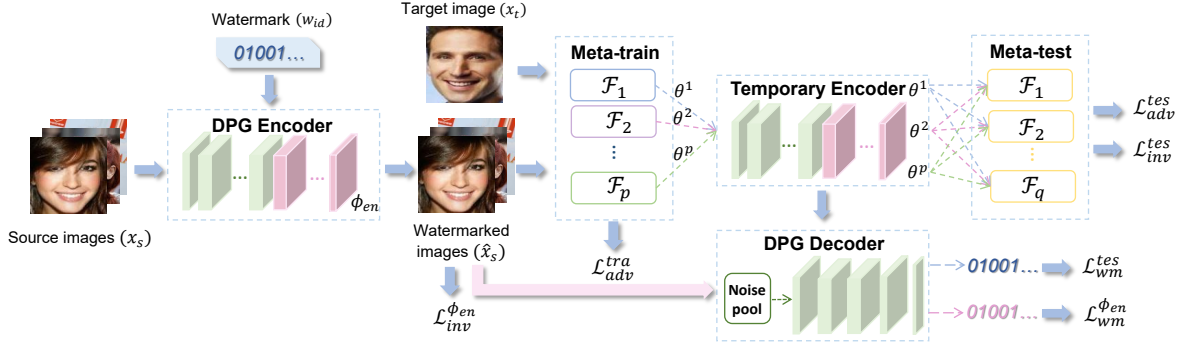


Fig. 2. The whole pipeline of the proposed DPG. The source image is first encoded with the original parameter encoder to obtain the watermarked image. The watermarked image then enters the meta-learning module for adversarial training using a temporary encoder and undergoes traceability optimization through the noise-pool-based watermark decoder.

### B. Multi-Task Compatible Meta-Optimization

The DPG encoder is associated with two distinct sub-tasks: 1) *encoding the watermark recoverably and invisibly*; 2) *adversarial encoding the watermark to deceive FR models*. Simultaneously, the decoder needs to accurately extract the watermark. DPG are optimized end-to-end to search for the global optimal solution. However, there are optimization conflicts between different tasks. Enhancing adversariality only under a single FR model or after simply ensemble FR models hinders watermark invisibility optimization, introducing more obvious perceptual artifacts to the watermarked image. Additionally, this adversarial enhancement is not effectively transferred to black-box models. Therefore, to enhance the transferability and mitigate this optimization conflict, we adopt a collaborative meta-optimization strategy compatible with multi-task. This strategy builds upon Model-Agnostic Meta-Learning (MAML) method [22] and further corrects the training errors of different tasks, seamlessly integrating into end-to-end training to aid overall optimization. The schematic diagram of model parameter updates in the overall optimization is shown in Figure 3.

We select  $P$  meta-training models and  $Q$  meta-testing models, initially calculating the adversarial loss under the meta-training models with the initial encoder parameters  $\phi_{en}$ :

$$\mathcal{L}_{adv}^{tra} = \sum_{p=1}^P \mathcal{L}_{adv}(\mathcal{F}_p(\hat{x}_s), \mathcal{F}_p(x_t) | \phi_{en}). \quad (8)$$

For each meta-training model, we calculate the gradient of the adversarial loss with respect to the encoder parameters based on the model, and update the temporary parameters  $\theta^p$  of the current encoder according to this gradient:

$$\theta^p \leftarrow \phi_{en} - \eta \nabla_{\phi_{en}} \mathcal{L}_{adv}^{tra}. \quad (9)$$

The encoder utilizes temporary parameters to generate the watermarked image  $\hat{x}_{s\_tes}$ :

$$\hat{x}_{s\_tes} = \mathcal{E}(x_s, w_{id} | \theta^p). \quad (10)$$

Temporary watermarked images are used to compute test errors on meta-testing models, assessing the meta-performance

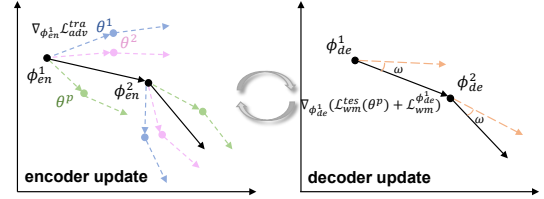


Fig. 3. Illustration of encoder and decoder co-optimization. The encoder optimizes towards a general direction through meta-optimization, while the decoder simultaneously adjusts its optimization direction based on the temporary parameters of the encoder.

across  $P$  tasks and refining the original optimization direction. The meta-testing adversarial loss  $\mathcal{L}_{meta}^{tes}$  is defined as:

$$\mathcal{L}_{adv}^{tes} = \sum_{p=1}^P \sum_{q=1}^Q \mathcal{L}_{adv}(\mathcal{F}_q(\hat{x}_{s\_tes}), \mathcal{F}_q(x_t) | \theta^p). \quad (11)$$

To ensure compatibility with the invisibility optimization task and further constrain image degradation due to adversarial enhancement, we concurrently calculate the invisibility loss  $\mathcal{L}_{inv}^{tes}$  based on  $\hat{x}_{s\_tes}$  under temporary parameters, unifying the gradient optimization direction:

$$\mathcal{L}_{inv}^{tes} = \frac{1}{PQ} \sum_{p=1}^P \sum_{q=1}^Q \mathcal{L}_{MSE}(\hat{x}_{s\_tes}, x_s | \theta^p), \quad (12)$$

the total invisibility loss  $\mathcal{L}_{inv}^{total}$  and total adversarial loss  $\mathcal{L}_{adv}^{total}$  during end-to-end updates are calculated as follows:

$$\mathcal{L}_{inv}^{total} = (\mathcal{L}_{inv}^{en} + \mathcal{L}_{inv}^{tes})/2. \quad (13)$$

$$\mathcal{L}_{adv}^{total} = \mathcal{L}_{adv}^{tra} + \mathcal{L}_{adv}^{tes}. \quad (14)$$

### C. Regularization-Enhanced Information Decoding

Online networks process uploaded images to conform to file storage and transmission standards. This processing significantly changes the watermark distribution and increases the difficulty of watermark extraction. Therefore, we design

a joint noise pool in front of the decoder, which includes differentiable JPEG compression ( $QF = 50$ ) and Gaussian noise ( $Var = 0.003$ ), enhancing the decoder robustness. We initially calculate the information loss of the watermarked image obtained under the original encoder parameters using BCE loss  $\mathcal{L}_{BCE}$ , as follows:

$$\mathcal{L}_{wm}^{\phi_{en}} = \mathcal{L}_{BCE}(w_{id}, \mathcal{D}(NP(\mathcal{E}(x_s, w_{id} | \phi_{en}))))). \quad (15)$$

The encoder and decoder interact synergistically during co-optimization, serving as mutual priors, as illustrated in Figure 3. To enhance cross-model gradient compatibility, we introduce an information regularization module. This module calculates information loss using the latest temporary update of the watermarked image, allowing it to further refine the optimization direction of the decoder based on the encoder:

$$\mathcal{L}_{wm}^{tes} = \mathcal{L}_{BCE}(w_{id}, \mathcal{D}(NP(\mathcal{E}(x_s, w_{id} | \theta^P))))). \quad (16)$$

The overall watermark information loss is calculated by:

$$\mathcal{L}_{wm}^{total} = \mathcal{L}_{wm}^{\phi_{en}} + \mathcal{L}_{wm}^{tes}. \quad (17)$$

The outer loop optimization of the model updates the encoder and decoder with adversarial loss, invisibility loss, and watermark information loss as joint optimization objectives. The total loss of DPG is calculated as follows:

$$\mathcal{L}_{DPG} = \lambda_{adv} \mathcal{L}_{adv}^{total} + \lambda_{inv} \mathcal{L}_{en}^{total} + \lambda_{wm} \mathcal{L}_{wm}^{total}, \quad (18)$$

where  $\lambda_{adv}$ ,  $\lambda_{en}$  and  $\lambda_{wm}$  are positive hyperparameters, and we empirically set them to 100, 0.05 and 0.05, respectively.

## V. EXPERIMENTS

### A. Experimental Settings

1) *Datasets*: We evaluate DPG on two commonly used large face image datasets: LFW [23] and CelebA [24]. The watermark message is 50 bits, sufficient to meet the requirements for representing identity in the real world. To meet the input size requirements of FR models, all images are initially processed through MTCNN [25] to extract facial regions and sampled to a size of  $112 \times 112$ .

2) *Implementation details*: The entire training process of DPG spans 2500 epochs with a batch size of 32. We empirically adjust the Adam optimizer with an initial learning rate of 0.00005 for stable training. We select various offline and online commercial victim FR models to evaluate the black-box transferability of DPG, including: 1) *Offline models*: IR152, IRSE50, MobileFace [20], FaceNet [26], ArcFace [20] based on IResNet100 [27] and CosFace [28] based on IResNet100. 2) *Online models*: Face++ [29] and Aliyun [30]. We alternately selected three models from them as white-box models for integrated training and sequentially obtained black-box test results on the remaining models as in [9], [10], [31], with the parameters set as  $P = 2$  and  $Q = 1$ .

3) *Comparisons*: DPG is the first watermarking method designed for FR models with both adversariality and traceability, and there is no similar work before. Thus, we first compare its adversariality with adversarial example methods: 1) *Patch-based methods*: Adv-Makeup [10], AdvHat [9]; 2) *Perturbation-based methods*: PGD [11], FGSM [12]. Simultaneously, we straightforwardly combine adversarial example methods with watermarking methods Hidden [7] and Fake-Tagger [14]. We embed watermarks directly into adversarial examples generated by PGD and FGSM, comparing adversariality and traceability to illustrate the advantages of DPG.

4) *Metrics*: We use SSIM [32] to evaluate the quality of images. Accuracy  $Acc$  is used to evaluate the watermark recovery accuracy of the watermarked image. we adopt Attack Success Rate (ASR) [33] for impersonation attack to evaluate adversariality, which is calculated through:

$$ASR = \frac{\sum_i^N \cos[\mathcal{F}(x_t^i), \mathcal{F}(\hat{x}_s^i)] > \tau}{N}, \quad (19)$$

where  $i$  represents the image index,  $N$  represents the total number of test images, and  $\tau$  represents the similarity threshold. The value of  $\tau$  will be set as the threshold at 0.01 FAR (False Acceptance Rate) for each victim FR model as most face recognition works do, i.e., IR152 (0.167), IRSE50 (0.241), MobileFace (0.302), Facenet (0.409), ArcFace (0.280) and CosFace (0.280) [10].

### B. Comparison with Baselines

To meet the challenges of the practical scenarios, where users may lack knowledge of the underlying structure and the specific training schemes of the FR models used by third-party databases, we focus on evaluating the defense method's performance against black-box models. To ensure that the generated adversarial images do not affecting normal usage, we controlled the average SSIM values of all adversarial images from different methods to be  $0.9 \pm 0.03$  in our experiments for fair comparison. As shown in Table II, DPG exhibits excellent adversariality and traceability simultaneously. It achieves optimal ASR on almost all evaluated black-box FR models, surpassing adversarial example methods that only possess adversariality. Moreover, DPG outperforms combination-based methods in both adversariality and traceability, especially on FaceNet, ArcFace, and CosFace, where watermark embedding significantly reduces the adversariality of the generated examples. Most importantly, DPG achieves two significant performances by training only one set of watermarking models, providing a more unified management approach for users or authorizers over models and images.

To assess the practical viability of the attack methods, we leverage the face comparison feature of online commercial FR models. We compared the generated adversarial images from different methods with the target facial images, and the platform provided confidence score indicating whether the two images belong to the same identity. We reported the Average Confidence Scores (ACS) for 100 images from the LFW dataset. As shown in Table III, DPG achieved the highest ACS while maintaining excellent traceability accuracy. This confirms the feasibility of DPG for practical deployment.

Datasets	Type	Method	IR152		IRSE50		ArcFace		MobileFace		FaceNet		CosFace	
			ASR	ACC										
LFW	Patch-based	Adv-Makeup	0.026	N/A	0.236	N/A	0.026	N/A	0.289	N/A	0.026	N/A	0.00	N/A
		AdvHat	0.017	N/A	0.187	N/A	0.000	N/A	0.215	N/A	0.008	N/A	0.000	N/A
	Perturbation-based	PGD	<u>0.311</u>	N/A	<u>0.788</u>	N/A	<u>0.367</u>	N/A	<b>0.755</b>	N/A	<u>0.155</u>	N/A	<u>0.266</u>	N/A
		FGSM	0.177	N/A	0.588	N/A	0.111	N/A	0.622	N/A	0.067	N/A	0.044	N/A
	Combination-based	PGD+Hidden	0.182	0.988	0.501	0.988	0.065	0.984	0.433	0.988	0.062	0.984	0.037	0.967
		FGSM+Hidden	0.109	0.988	0.310	0.988	0.011	0.983	0.299	0.988	0.011	0.983	0.015	0.983
		PGD+FakeTagger	0.265	<u>0.991</u>	0.532	<u>0.989</u>	0.050	<u>0.995</u>	0.483	<u>0.989</u>	0.040	<u>0.991</u>	0.030	<u>0.986</u>
	Watermark-based	FGSM+FakeTagger	0.112	0.986	0.350	0.986	0.020	0.988	0.391	0.986	0.010	0.988	0.020	0.988
		<b>DPG (ours)</b>	<b>0.326</b>	<b>0.992</b>	<b>0.810</b>	<b>0.997</b>	<b>0.381</b>	<b>0.996</b>	<u>0.716</u>	<b>0.997</b>	<b>0.643</b>	<b>0.994</b>	<b>0.355</b>	<b>0.996</b>
	CelebA	Patch-based	Adv-Makeup	0.087	N/A	0.193	N/A	0.017	N/A	0.000	N/A	0.421	N/A	0.00
AdvHat			0.017	N/A	0.072	N/A	0.000	N/A	0.071	N/A	0.000	N/A	0.000	N/A
Perturbation-based		PGD	<u>0.400</u>	N/A	<b>0.660</b>	N/A	<b>0.450</b>	N/A	<b>0.720</b>	N/A	<u>0.270</u>	N/A	<u>0.378</u>	N/A
		FGSM	0.180	N/A	0.420	N/A	0.220	N/A	0.600	N/A	0.100	N/A	0.180	N/A
Combination-based		PGD+Hidden	0.132	0.978	0.291	0.983	0.141	0.957	0.181	0.979	0.143	0.960	0.090	0.960
		FGSM+Hidden	0.122	0.975	0.171	0.975	0.080	0.968	0.100	0.958	0.030	0.968	0.000	0.966
		PGD+FakeTagger	0.376	<u>0.986</u>	0.380	<u>0.993</u>	0.240	0.988	0.364	<u>0.993</u>	0.171	0.984	0.290	0.986
Watermark-based		FGSM+FakeTagger	0.311	<u>0.986</u>	0.240	0.992	0.111	<u>0.989</u>	0.281	0.992	0.060	<u>0.992</u>	0.080	<u>0.987</u>
		<b>DPG (ours)</b>	<b>0.433</b>	<b>0.998</b>	<u>0.635</u>	<b>0.998</b>	<u>0.375</u>	<b>0.995</b>	<u>0.679</u>	<b>0.997</b>	<b>0.318</b>	<b>0.995</b>	<b>0.393</b>	<b>0.998</b>

TABLE II

ASR AND ACC RESULTS OF BLACK-BOX IMPERSONATION ATTACK ON THE LFW AND CELEBA DATASETS. *N/A* INDICATES THAT THE METHOD CANNOT ACHIEVE THIS EFFECT AND LACKS SUPPORTING DATA. THE BEST RESULTS ARE EMPHASIZED IN BOLD, THE SECOND-BEST RESULTS ARE UNDERScoreD.

Type	Method	Face++		Aliyun	
		ACS	ACC	ACS	ACC
Patch-based	Adv-makeup	52.320	N/A	6.603	N/A
	Adv-Hat	48.030	N/A	3.493	N/A
Perturbation-based	PGD	<u>65.000</u>	N/A	<u>41.517</u>	N/A
	FGSM	58.490	N/A	27.780	N/A
Combination-based	PGD+Hidden	49.748	0.983	27.067	0.993
	FGSM+Hidden	45.889	0.975	22.095	0.975
	PGD+FakeTagger	54.370	<u>0.993</u>	33.572	<u>0.993</u>
Watermark-based	FGSM+FakeTagger	46.325	0.992	22.537	0.992
	<b>DPG (ours)</b>	<b>65.491</b>	<b>0.998</b>	<b>43.945</b>	<b>0.998</b>

TABLE III

ACS AND ACC RESULTS ON ONLINE COMMERCIAL FR SYSTEMS.



Fig. 4. Visual comparison of adversarial examples and watermarked images obtained by different methods on the CelebA dataset.

### C. Robustness Analysis

Online platforms often process images to conform to uniform transmission standards. Therefore, we evaluate the adversarial robustness and traceability robustness of the methods after applying Gaussian noise (GN), JPEG compression (JPEG), or resizing (Resize), as shown in Table IV. DPG maintains optimal performance even after various image processing, surpassing dedicated adversarial attack methods by up to 58% in adversarial robustness and outperforming combination-based methods in traceability robustness. This robustness advantage can be attributed to two factors. Firstly, unlike adversarial attacks that directly overlay gradients, DPG embeds watermarks in the deep feature space of the carrier.

Additionally, DPG synergistically optimizes the encoder and decoder, introducing adversarial attack to increase the output dimensions of the model. [21] has confirmed that multitask learning, especially the joint optimization of tasks with low correlation, significantly enhances model robustness.

### D. Visualization and Analysis

We present the visual results of different methods using samples covering various genders, ages, and degrees of facial occlusion, as shown in Figure 4. Patch-based methods rely on significant semantic modifications to images. Adv-Makeup has limitations for images with occluded eyes. Perturbation-based methods produce adversarial examples with regular noise patterns, easy to be discovered and defended by adversaries. DPG-generated watermarked images exhibit only differences in overall hue, without noticeable artifacts. Additionally, we use Grad-CAM [34] visualization to illustrate the gradient responses of FGSM and DPG under black-box and white-box models. As shown in Figure 5, FGSM and DPG both modify gradient responses in the white-box model. While FGSM overfit to modifications in the region of interest of the white-box model, including the background, resulting in poor transferability to black-box models. DPG encodes more universal adversarial features of the carrier, focusing on crucial facial regions, and effectively transfers these adversariality to the black-box model.

### E. Ablation Study

To illustrate the influence of incorporating the meta-optimization strategy compatible with multiple tasks in end-to-end optimization on the comprehensive performance of DPG, we present the results of ablation experiments in Table V. Meta-optimization strategy in DPG simultaneously enhances image quality and ASR. This is attributed to the encoder quickly adapting to new tasks with minimal gradient updates

Processing	Parameters	Type	Method	IR152		IRSE50		ArcFace		MobileFace		FaceNet		CosFace	
				ASR	ACC										
GN	0.003	Patch-based	Adv-Makeup	0.026	N/A	0.263	N/A	0.026	N/A	0.289	N/A	0.026	N/A	0.000	N/A
			AdvHat	0.017	N/A	0.008	N/A	0.000	N/A	0.071	N/A	0.000	N/A	0.000	N/A
		Perturbation-based	PGD	0.191	N/A	<u>0.465</u>	N/A	0.011	N/A	<u>0.372</u>	N/A	0.015	N/A	0.011	N/A
			FGSM	0.150	N/A	0.292	N/A	0.017	N/A	0.305	N/A	0.000	N/A	0.000	N/A
		Combination-based	PGD+Hidden	0.211	0.629	0.424	0.629	<u>0.055</u>	0.632	0.365	0.629	<u>0.033</u>	0.632	0.016	0.632
			FGSM+Hidden	0.113	0.633	0.145	0.633	0.000	0.636	0.312	0.633	0.011	0.636	0.000	0.636
			PGD+FakeTagger	0.220	0.971	0.410	0.971	0.023	0.961	0.341	0.971	0.017	0.961	0.022	0.961
			FGSM+FakeTagger	0.103	0.970	0.312	0.970	0.013	<u>0.963</u>	0.300	0.970	0.011	<u>0.963</u>	<u>0.024</u>	<u>0.963</u>
		Watermark-based	<b>DPG (ours)</b>	<b>0.265</b>	<b>0.975</b>	<b>0.725</b>	<b>0.987</b>	<b>0.308</b>	<b>0.979</b>	<b>0.695</b>	<b>0.987</b>	<b>0.563</b>	<b>0.975</b>	<b>0.311</b>	<b>0.985</b>
		JPEG	30	Patch-based	Adv-Makeup	0.000	N/A	0.052	N/A	0.000	N/A	0.131	N/A	0.000	N/A
AdvHat	0.008				N/A	0.008	N/A	0.000	N/A	0.035	N/A	0.000	N/A	0.000	N/A
Gradient-based	PGD			0.244	N/A	<u>0.523</u>	N/A	<u>0.051</u>	N/A	<u>0.480</u>	N/A	0.026	N/A	0.033	N/A
	FGSM			0.205	N/A	0.371	N/A	0.013	N/A	0.375	N/A	0.022	N/A	0.011	N/A
Combination-based	PGD+Hidden			<u>0.261</u>	0.654	0.513	0.654	0.032	0.662	0.412	0.654	0.030	0.662	<u>0.045</u>	0.662
	FGSM+Hidden			0.119	0.686	0.280	0.686	0.000	0.655	0.295	0.686	<u>0.035</u>	0.655	0.016	0.655
	PGD+FakeTagger			0.260	0.886	0.463	0.886	0.040	<u>0.883</u>	0.440	<u>0.898</u>	0.021	<u>0.883</u>	0.029	<u>0.883</u>
	FGSM+FakeTagger			0.119	<u>0.887</u>	0.310	<u>0.887</u>	0.016	<u>0.883</u>	0.360	0.887	0.022	<u>0.883</u>	0.011	<u>0.883</u>
Watermark-based	<b>DPG (ours)</b>			<b>0.272</b>	<b>0.967</b>	<b>0.655</b>	<b>0.958</b>	<b>0.286</b>	<b>0.983</b>	<b>0.736</b>	<b>0.967</b>	<b>0.587</b>	<b>0.983</b>	<b>0.398</b>	<b>0.980</b>
Resize	1/2			Patch-based	Adv-Makeup	0.026	N/A	0.236	N/A	0.026	N/A	0.289	N/A	0.026	N/A
		AdvHat	0.008		N/A	0.008	N/A	0.000	N/A	0.003	N/A	0.000	N/A	0.000	N/A
		Perturbation-based	PGD	0.233	N/A	0.380	N/A	<u>0.039</u>	N/A	0.433	N/A	0.017	N/A	<u>0.028</u>	N/A
			FGSM	0.200	N/A	0.310	N/A	0.000	N/A	0.351	N/A	0.016	N/A	0.000	N/A
		Combination-based	PGD+Hidden	<u>0.241</u>	0.691	<u>0.411</u>	0.691	0.023	0.641	<u>0.444</u>	0.691	<u>0.022</u>	0.641	0.023	0.641
			FGSM+Hidden	0.109	0.714	0.312	0.714	0.000	0.721	0.333	0.714	0.011	0.721	0.000	0.721
			PGD+FakeTagger	0.203	0.986	0.336	0.986	0.025	<u>0.988</u>	0.425	0.986	0.011	<u>0.988</u>	0.016	<b>0.988</b>
			FGSM+FakeTagger	0.137	<u>0.987</u>	0.246	<u>0.987</u>	0.000	0.986	0.361	<u>0.987</u>	0.011	0.986	0.000	0.986
		Watermark-based	<b>DPG (ours)</b>	<b>0.255</b>	<b>0.990</b>	<b>0.584</b>	<b>0.990</b>	<b>0.211</b>	<b>0.989</b>	<b>0.688</b>	<b>0.990</b>	<b>0.408</b>	<b>0.993</b>	<b>0.253</b>	<b>0.988</b>

TABLE IV

ASR AND ACC RESULTS AFTER VARIOUS IMAGE PROCESSING OPERATIONS. THE TESTING DATASET USED IS THE LFW DATASET.

Method	IR152		IRSE50		ArcFace		MobileFace		FaceNet		CosFace	
	ASR	SSIM										
w/o Meta	0.136	0.867	0.522	0.873	0.193	0.867	0.601	0.859	0.496	0.865	0.227	0.873
DPG	<b>0.326</b>	<b>0.903</b>	<b>0.810</b>	<b>0.896</b>	<b>0.381</b>	<b>0.911</b>	<b>0.716</b>	<b>0.911</b>	<b>0.643</b>	<b>0.898</b>	<b>0.355</b>	<b>0.913</b>

TABLE V

ABLATION EXPERIMENT. **W/O Meta** INDICATES DPG IS TRAINED WITH A DIRECT ENSEMBLE OF FR MODELS, WITHOUT META-OPTIMIZATION.

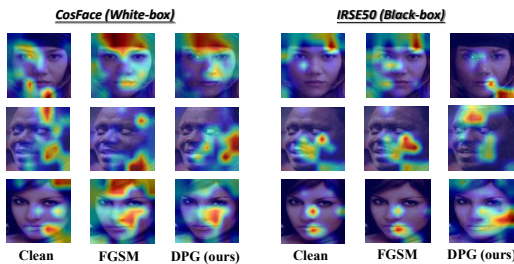


Fig. 5. Visualization using Grad-CAM produces attention maps on CosFace model and IRSE50 model.

during meta-optimization, acquiring universal adversarial features for the carrier against unknown victim models. This avoids excessive reliance on penalizing image quality to enhance adversarial characteristics.

## VI. CONCLUSION

To address the limitations of existing privacy protection methods, we propose DPG, the first method that protects facial image privacy from both adversarial and traceable perspectives. We first propose an information-guided adversarial attack strategy, which guides recognizable features of the image to deviate from the source identity features through an identity-specific watermark. Then we introduce a meta-optimization strategy that is compatible with multiple tasks to solve the

optimization conflict between transferability and watermark invisibility. Experiments confirm the significant transferability, traceability and robustness of DPG on the SOTA FR models.

## REFERENCES

- [1] J. Liu, C. P. Lau, and R. Chellappa, “Diffprotect: Generate adversarial examples with diffusion models for facial privacy protection,” *arXiv preprint arXiv:2305.13625*, 2023.
- [2] L. Yang, Q. Song, and Y. Wu, “Attacks on state-of-the-art face recognition using attentional adversarial attack generative network,” *Multimedia tools and applications*, vol. 80, pp. 855–875, 2021.
- [3] X. Wei, Y. Guo, J. Yu, and B. Zhang, “Simultaneously optimizing perturbations and positions for black-box adversarial patch attacks,” *IEEE transactions on pattern analysis and machine intelligence*, 2022.
- [4] Z. Li, B. Yin, T. Yao, J. Guo, S. Ding, S. Chen, and C. Liu, “Sibling-attack: Rethinking transferable adversarial attacks against face recognition,” in *Proceedings of the IEEE/CVF Conference on Computer Vision and Pattern Recognition (CVPR)*, June 2023, pp. 24 626–24 637.
- [5] Y. Dong, H. Su, B. Wu, Z. Li, W. Liu, T. Zhang, and J. Zhu, “Efficient decision-based black-box adversarial attacks on face recognition,” *2019 IEEE/CVF Conference on Computer Vision and Pattern Recognition*, pp. 7706–7714, 2019.
- [6] S. Jia, B. Yin, T. Yao, S. Ding, C. Shen, X. Yang, and C. Ma, “Adv-attribute: Inconspicuous and transferable adversarial attack on face recognition,” *Advances in Neural Information Processing Systems*, vol. 35, pp. 34 136–34 147, 2022.
- [7] J. Zhu, R. Kaplan, J. Johnson, and L. Fei-Fei, “Hidden: Hiding data with deep networks,” in *Proceedings of the European conference on computer vision*, 2018, pp. 657–672.
- [8] M. Sharif, S. Bhagavatula, L. Bauer, and M. K. Reiter, “A general framework for adversarial examples with objectives,” *ACM Transactions on Privacy and Security (TOPS)*, vol. 22, no. 3, pp. 1–30, 2019.
- [9] S. Komkov and A. Petiushko, “Advhat: Real-world adversarial attack on arface face id system,” in *2020 25th International Conference on Pattern Recognition*. IEEE, 2021, pp. 819–826.
- [10] B. Yin, W. Wang, T. Yao, J. Guo, Z. Kong, S. Ding, J. Li, and C. Liu, “Adv-makeup: A new imperceptible and transferable attack on face recognition,” *arXiv preprint arXiv:2105.03162*, 2021.
- [11] A. Madry, A. Makelov, L. Schmidt, D. Tsipras, and A. Vladu, “Towards deep learning models resistant to adversarial attacks,” *arXiv preprint arXiv:1706.06083*, 2017.

- [12] I. J. Goodfellow, J. Shlens, and C. Szegedy, "Explaining and harnessing adversarial examples," *arXiv preprint arXiv:1412.6572*, 2014.
- [13] Y. Zhong and W. Deng, "Towards transferable adversarial attack against deep face recognition," *IEEE Transactions on Information Forensics and Security*, vol. 16, pp. 1452–1466, 2020.
- [14] R. Wang, F. Juefei-Xu, M. Luo, Y. Liu, and L. Wang, "Faketagger: Robust safeguards against deepfake dissemination via provenance tracking," in *Proc. 29th ACM Int. Conf. Multimedia*, 2021, pp. 3546–3555.
- [15] N. Yu, V. Skripniuk, S. Abdelnabi, and M. Fritz, "Artificial fingerprinting for generative models: Rooting deepfake attribution in training data," in *Proceedings of the IEEE/CVF International Conference on Computer Vision*, 2021, pp. 14 448–14 457.
- [16] X. Jia, X. Wei, X. Cao, and X. Han, "Adv-watermark: A novel watermark perturbation for adversarial examples," in *Proc. 28th ACM Int. Conf. Multimedia*, 2020, pp. 1579–1587.
- [17] H. Jiang, J. Yang, G. Hua, L. Li, Y. Wang, S. Tu, and S. Xia, "Fawa: Fast adversarial watermark attack," *IEEE Trans. on Comput.*, pp. 1–1, 2021.
- [18] Z. Jia, H. Fang, and W. Zhang, "Mbrs: Enhancing robustness of dnn-based watermarking by mini-batch of real and simulated jpeg compression," in *Proceedings of the 29th ACM international conference on multimedia*, 2021, pp. 41–49.
- [19] S. Woo, J. Park, J.-Y. Lee, and I. S. Kweon, "Cbam: Convolutional block attention module," in *Proc. Eur. Conf. Comput. Vis. (ECCV)*, 2018, pp. 3–19.
- [20] J. Deng, J. Guo, N. Xue, and S. Zafeiriou, "Arcface: Additive angular margin loss for deep face recognition," in *Proceedings of the IEEE/CVF conference on computer vision and pattern recognition*, 2019, pp. 4690–4699.
- [21] C. Mao, A. Gupta, V. Nitin, B. Ray, S. Song, J. Yang, and C. Vondrick, "Multitask learning strengthens adversarial robustness," in *Computer Vision—ECCV 2020: 16th European Conference, Glasgow, UK, August 23–28, 2020, Proceedings, Part II 16*, 2020, pp. 158–174.
- [22] C. Finn, P. Abbeel, and S. Levine, "Model-agnostic meta-learning for fast adaptation of deep networks," in *International conference on machine learning*, 2017, pp. 1126–1135.
- [23] G. B. Huang, M. Mattar, T. Berg, and E. Learned-Miller, "Labeled faces in the wild: A database for studying face recognition in unconstrained environments," in *Workshop on faces in 'Real-Life' Images: detection, alignment, and recognition*, 2008.
- [24] Z. Liu, P. Luo, X. Wang, and X. Tang, "Deep learning face attributes in the wild," in *Proceedings of the IEEE international conference on computer vision*, 2015, pp. 3730–3738.
- [25] K. Zhang, Z. Zhang, Z. Li, and Y. Qiao, "Joint face detection and alignment using multitask cascaded convolutional networks," *IEEE Signal Processing Letters*, vol. 23, no. 10, pp. 1499–1503, 2016.
- [26] M. Sharif, S. Bhagavatula, L. Bauer, and M. K. Reiter, "Accessorize to a crime: Real and stealthy attacks on state-of-the-art face recognition," in *Proceedings of the 2016 acm sigsac conference on computer and communications security*, 2016, pp. 1528–1540.
- [27] I. C. Duta, L. Liu, F. Zhu, and L. Shao, "Improved residual networks for image and video recognition," in *2020 25th International Conference on Pattern Recognition (ICPR)*. IEEE, 2021, pp. 9415–9422.
- [28] H. Wang, Y. Wang, Z. Zhou, X. Ji, D. Gong, J. Zhou, Z. Li, and W. Liu, "Cosface: Large margin cosine loss for deep face recognition," in *Proceedings of the IEEE conference on computer vision and pattern recognition*, 2018, pp. 5265–5274.
- [29] MEGVII, "In <https://www.faceplusplus.com.cn/>," 2021.
- [30] Aliyun, "<https://cn.aliyun.com/>," 2019.
- [31] S. Hu, X. Liu, Y. Zhang, M. Li, L. Y. Zhang, H. Jin, and L. Wu, "Protecting facial privacy: Generating adversarial identity masks via style-robust makeup transfer," in *Proceedings of the IEEE/CVF Conference on Computer Vision and Pattern Recognition*, 2022, pp. 15 014–15 023.
- [32] Z. Wang, A. Bovik, H. Sheikh, and E. Simoncelli, "Image quality assessment: From error visibility to structural similarity," *IEEE Trans. Image Process.*, p. 600–612, Apr 2004.
- [33] D. Deb, J. Zhang, and A. K. Jain, "Advfaces: Adversarial face synthesis," in *2020 IEEE International Joint Conference on Biometrics*, 2020, pp. 1–10.
- [34] R. R. Selvaraju, M. Cogswell, A. Das, R. Vedantam, D. Parikh, and D. Batra, "Grad-cam: Visual explanations from deep networks via gradient-based localization," in *Proceedings of the IEEE international conference on computer vision*, 2017, pp. 618–626.